Geotechnical Testing Journal

doi:10.1520/GTJ20160069 / Vol. 40 / No. 3 / May 2017 / available online at www.astm.org

# TECHNICAL NOTE

S. M. Fattahi,[1] A. Soroush,[2] and P. T. Shourijeh[3]

# The Hole Erosion Test: A Comparison of Interpretation Methods

**Reference**

Fattahi, S. M., Soroush, A., and Shourijeh, P. T., "The Hole Erosion Test: A Comparison of Interpretation Methods," *Geotechnical Testing Journal*, Vol. 40, No. 3, 2017, pp. 494–505, http://dx.doi.org/10.1520/GTJ20160069. ISSN 0149-6115

**ABSTRACT**

The hole erosion test (HET) is widely performed for determining soil erosion characteristics; viz. critical shear stress, erosion rate coefficient, and erosion rate index. Refinements to measurement/estimation of water head drop in the hole through the specimen, which is essential in accurate interpretation of HET, were proposed. Particular attention was devoted to head losses in the entrance/exit of flow to/from the hole in the specimen, and any changes in the hole's entrance geometry. Soil erodibility parameters of 13 core soils obtained in HET through previously available methods, and the new proposed technique were described and compared. Results suggested that, although differences are observed between erosion rate coefficient and critical shear stress from different methods, the erosion rate indices were close, in so far as the interpretation methods manifest an identical classification for soil erosion propensity.

**Keywords**

internal erosion, concentrated leak, Hole Erosion Test (HET), erosion rate, critical shear stress

Manuscript received April 6, 2016; accepted for publication November 30, 2016; published online February 16, 2017.

[1] Dept. of Civil & Environmental Engineering, Amirkabir Univ. of Technology, Tehran, Iran

[2] Dept. of Civil & Environmental Engineering, Amirkabir Univ. of Technology, Tehran, Iran (Corresponding author), e-mail: soroush@aut.ac.ir

[3] Dept. of Civil & Environmental Engineering, Shiraz Univ. of Technology, Shiraz, Iran

## Nomenclature

$C_e$ = coefficient of soil erosion (s/m)
$f_L$ = friction factor in laminar flow conditions ($Ns/m^3$)
$f_T$ = friction factor in turbulent flow conditions ($Ns^2/m^4$)
$g$ = acceleration of gravity ($m/s^2$)
$h_d$ = downstream hydraulic head (m)
$h_{ent}$ = head loss in hole entrance (m)
$h_{ext}$ = head loss in hole exit (m)

$h_f$ = friction head loss along the axial hole (m)
$h_u$ = upstream hydraulic head (m)
$I$ = erosion rate index
$i$ = flow gradient along the hole
$K_{ent}$ = entrance head loss coefficient
$K_{ext}$ = exit head loss coefficient
$L$ = length of axial hole (m)
$LL$ = liquid limit (%)
$\nu$ = kinematic viscosity ($m^2/s$)
$p$ = pressure ($kN/m^2$)
$PI$ = plasticity index (%)
$Q$ = flow rate ($m^3/s$)
$R_e$ = Reynolds number
$t$ = elapsed time (s)
$t_f$ = test termination (end) time (s)
$V_d$ = mean flow velocity in downstream chamber (m/s)
$V_h$ = mean flow velocity in axial hole (m/s)
$V_u$ = mean flow velocity in upstream chamber (m/s)
$w_{opt}$ = optimum water content (%)
$z$ = elevation head (m)
$\Delta H$ = total energy head loss (m)
$\Delta h$ = hydraulic head difference across the soil specimen (m)
$\dot{\varepsilon}_t$ = rate of erosion per unit surface area of hole at time t ($kg/s/m^2$)
$\phi_d$ = downstream flow chamber diameter (m)
$\phi_u$ = upstream flow chamber diameter (m)
$\phi_t$ = estimated mean diameter of axial hole at time $t$ (m)
$\theta$ = entrance funnel shape angle
$\rho_d$ = dry density of soil ($kg/m^3$)
$\rho_w$ = density of water ($kg/m^3$)
$\tau_c$ = critical shear stress for soil erosion ($N/m^2$)
$\tau_t$ = shear stress exerted by eroding fluid at time $t$ ($N/m^2$)

## Introduction

Internal erosion from concentrated leaks occurs when water flows in an opening, crack, or deficiency in earth structures (ICOLD 2016). Consequently, the crack transmits water akin to a pipe, and soil particles are eroded due to hydraulic shear stresses exerted (ICOLD 2013). A well-known and very dangerous type of concentrated leak is erosion in cracks through impervious cores of embankment dams (Bonelli 2013). In such cases, the erodibility of core materials has significant influence on initiation and progression of internal erosion (Foster et al. 2000).

The hole erosion test (HET), developed by Wan and Fell (2002, 2004a, 2004b), is a comparatively simple, fast, and repeatable index test to study soil erosion from concentrated leaks (ICOLD 2016). This test includes a reconstituted or undisturbed soil specimen in which a 6 mm-diameter longitudinal hole is performed prior to testing. The prepared specimen is then subjected to head or flux controlled flow, while hydraulic conditions (flow rate, water head, etc.) in addition to any hole enlargement, are monitored in order to determine erodibility characteristics.

**TABLE 1** Qualitative description of erosion rate based on erosion rate index- Wan and Fell (2002, 2004a).

| Group No. | Erosion Rate Index ($I$) | Description |
|---|---|---|
| 1 | <2 | Extremely rapid |
| 2 | 2–3 | Very rapid |
| 3 | 3–4 | Moderately rapid |
| 4 | 4–5 | Moderately slow |
| 5 | 5–6 | Very slow |
| 6 | >6 | Extremely slow |

In the HET soil erosion is defined as $\dot{\varepsilon}_t = C_e(\tau_t - \tau_c)$ where, $\dot{\varepsilon}_t$ = rate of erosion per unit surface area of hole at time $t$ ($kg/s/m^2$), $C_e$ = coefficient of soil erosion (s/m), $\tau_t$ = hydraulic shear stress exerted by eroding fluid to hole surface area at time $t$ ($N/m^2$), and $\tau_c$ = critical shear stress, that is minimum hydraulic shear stress for erosion initiation ($N/m^2$). As seen in **Table 1**, soil erosion propensity is designated by the erosion rate index, $I$, defined as $I = -\log C_e$ (Wan and Fell 2002).

The erosion rate- from the hole- is estimated by (Wan and Fell 2002):

$$\dot{\varepsilon}_t = \frac{\rho_d}{2}\frac{d\phi_t}{dt} \tag{1}$$

where:

$\rho_d$ = soil dry density ($kg/m^3$), and
$d\phi_t/dt$ = change in hole diameter with time (m/s).

The hole diameter is calculated from pipe hydraulics as the following equations (Wan and Fell 2002):

$$\phi_t = \begin{cases} \left(\dfrac{16QLf_L}{\pi\rho_w g h_f}\right)^{\frac{1}{2}} Laminar\ Flow \\ \left(\dfrac{64Q^2Lf_T}{\pi^2\rho_w g h_f}\right)^{\frac{1}{5}} Turbulent\ Flow \end{cases} \tag{2}$$

where:

$\phi_t$ = estimated mean diameter of hole at time $t$ (m),
$Q$ = flow rate ($m^3/s$),
$L$ = length of axial hole (m),
$\rho_w$ = water density ($kg/m^3$),
$g$ = acceleration of gravity ($m/s^2$),
$h_f$ = friction head loss along axial hole (m), and
$f_L$ and $f_T$ = friction factors of hole periphery in laminar ($Ns/m^3$) and turbulent ($Ns^2/m^4$) flow conditions, respectively.

The flow is turbulent for Reynolds number, $R_e$, higher than 2000 (Wahl et al. 2008a). Note that $R_e = V_h\phi_t/\nu$, where $V_h$ = flow velocity in hole (m/s), $\phi_t$ = hole diameter (m), and

$\nu$ = water's kinematic viscosity ($m^2/s$). Exact measurements of $\phi_t$, are possible only at the beginning and end of tests, from which the initial and final friction factors may be back-calculated (cf. Eq 2). Throughout the test duration, logical estimations of $f_L$ and $f_T$ are prerequisite for mathematical calculation of $\phi_t$. It is assumed that $f_L$ and $f_T$ vary in linear proportion to $(Q/h_f)^{1/3}$ and $(Q^2/h_f)^{1/5}$ for laminar and turbulent flow, respectively, in-between their initial ($t = 0$), and final ($t = t_f$) values (Farrar et al. 2007; Wahl et al. 2008a, 2008b).

The boundary shear stress, $\tau_t$, exerted to the hole periphery, is directly related to hydraulic gradient, $i = h_f/L$, along the hole; that is (Wan and Fell 2002):

$$\tau_t = \rho_w g i \frac{\phi_t}{4} \quad (3)$$

The various simplifying assumptions and limitations of the HET procedure and interpretation method, have led to attempts by researchers to modify/refine the HET test.

Lim (2006) pointed to some problems of the HET and proposed modifications to specimen preparation, friction factors estimations, and test interpretation in case of slaking. Farrar et al. (2007) and Wahl et al. (2008a, 2008b) modified the HET apparatus and test setup, and also discussed factors effective in interpreting HET results, viz. curve-fitting procedures, erosion regimes (delayed or non-delayed), laminar versus turbulent flow, friction factor variation, and determination of final hole diameter.

Luthi (2011) and Luthi et al. (2012) presented a new HET configuration, termed HET-P, wherein incorporating a Pitot tube provides accurate measurement of total energy head and relevant losses. **Fig. 1** schematically shows the Pitot configuration in HET-P apparatus.

Reiffesteck et al. (2006) proposed effluent turbidity assessment for interpreting HET results. This approach is versatile, yet requires sophisticated/expensive equipment. Researchers such as Chevalier (2011), Chevalier et al. (2012), Benahmed and Bonelli (2012), and Haghighi et al. (2012) opted to use turbidity assessments in studying soil erosion.

In addition to laboratory proceedings, a number of researchers studied HET analytically and numerically. Bonelli et al. (2006) and Bonelli and Brivois (2008) proposed a numerical erosion model that correlates a dimensionless hole radius with critical shear stress, hydraulic gradient, and a dimensionless test time, enabling estimation of erosion characteristics without the need for interpolating hole diameter. Boukhemacha (2009) and Boukhemacha et al. (2013) presented a mathematical model for piping erosion; this model is derived from pipe flow equations, soil detachment and mass conservation laws, and may be written into an analytical radius-time equation in case of a constant pressure drop. Marot et al. (2011) and

**FIG. 1**

Schematic illustration of flow conditions in HET apparatus with Pitot-tube (Not to scale); redrawn/reworked after Luthi (2011) and Riha and Jandora (2014).

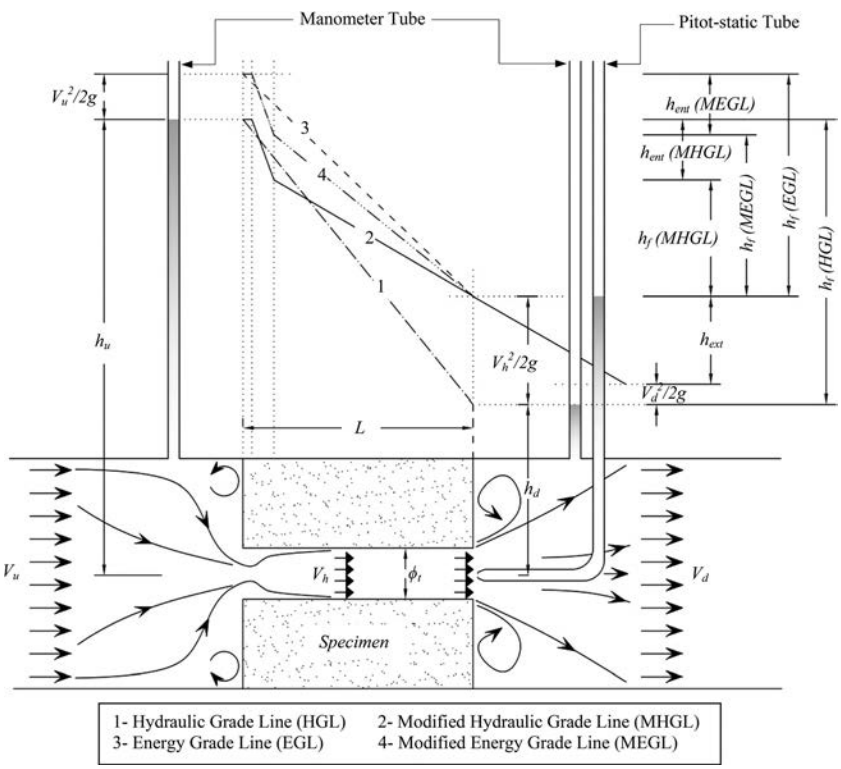

Regazzoni and Marot (2013) proposed a delicately balanced equation for fluid energy dissipation (considering identical upstream and downstream velocities) and eroded mass measurements in HET. Kissi et al. (2012), Riha and Jondora (2014), and Mercier et al. (2015) incorporated Computational Fluid Dynamics (CFD) software to analyze the HET.

The techniques employed for analyzing HET data, which depend on available equipment and measurements, stem from various fundamental theoretical assumptions that deserve precise pondering prior to application. Different methods for interpreting HET data may have merits and limitations, depending on soil type and erosion severity.

This treatment aims to refine the method from which water head drop (i.e., $h_f$) in the hole through the specimen is determined. This head drop is essential in accurate estimation/calculation of shear stresses exerted by eroding water flow on the walls of the hole, and in turn determination of principal soil erosion parameters, that are critical shear stress, $\tau_c$, and erosion rate coefficient, $C_e$. To this end, soil erodibility parameters of 13 core soils obtained in HET through previously available methods, and the new proposed technique are described and compared.

## Flow Hydraulics in HET

Considering the center flow line through the HET apparatus in **Fig. 1**, the conservation of energy, configured by Bernoulli's law, requires that (Luthi 2011; Bonelli 2013):

$$\underbrace{\left(\overbrace{\frac{p_u}{\rho_w g}}^{h_u} + z_u + \frac{V_u^2}{2g}\right)}_{H_u} = \underbrace{\left(\overbrace{\frac{p_d}{\rho_w g}}^{h_d} + z_d + \frac{V_d^2}{2g}\right)}_{H_d} + \Delta H \tag{4}$$

where:

$p$ = pressure,
$\rho_w$ = water density,
g = acceleration of gravity,
$V$ = mean flow velocity,
z = elevation head,
$h$ = hydraulic head,
$H$ = total energy head, and
$\Delta H$ = energy head loss from specimen's upstream to downstream, and connotations of $u$ and $d$ represent, respectively, the specimen's upstream and downstream. Apparently, $p/\rho_w g$ and $V^2/2g$ define the pressure and velocity heads, respectively.

The energy head loss, i.e., $\Delta H = H_u - H_d$, of flow passing through the hole from the specimen's upstream to downstream, consists of three parts (Riha and Jondora 2014; Bonelli 2013), hence:

$$\Delta H = h_{ent} + h_{ext} + h_f \tag{5}$$

where $h_{ent}$, $h_{ext}$, and $h_f$ are head losses in the entrance, exit and along the hole in specimen, respectively (cf. **Fig. 1**). The followings provide detailed description of the head losses:

### $h_{ent}$ or Head Loss Upon Flow Entrance to Hole

At the hole's entrance the cross-sectional area of flow reduces to a minimum, that is smaller than the hole. This phenomenon is known as "vena contrata," after which the stream widens to fill the hole. A fraction of the velocity head that is lost as a result of stream turbulence, is defined by (Riha and Jondora 2014; Potter et al. 2011):

$$h_{ent} = K_{ent}\left(\frac{V_h^2}{2g}\right) \tag{6}$$

where:

$V_h$ = flow velocity in hole, and
$K_{ent}$ = entrance head loss coefficient.

The graph in **Fig. 2**, presented by Okiishi et al. (2006), may be used to determine $K_{ent}$. Accordingly, $h_{ent} \leq 0.5 V_h^2/2g$ and this dissipation occurs between the "vena contrata" up-until the point when a uniform stream flow fills the hole (cf. **Fig. 1**). It is worthwhile noting that from continuity $V_h$ is much higher than $V_u$, hence; $h_{ent} > V_u^2/2g$ (cf. **Fig. 1**). The upstream hole end in erodible soil specimens usually deforms into a bevel/funnel-shaped entry during HET. Nonetheless, $h_{ent}$ would still be significant since the bevel-shaped hole is small in dimension compared to the upstream flow chamber diameter, hence the stream line would experience sudden contraction (Riha and Jondora 2014).

### $h_{ext}$ or Head Loss Upon Flow Exit From Hole

As illustrated in **Fig. 1**, at the hole's exit, stream flow from a smaller pipe (hole) into a larger pipe (downstream chamber) experiences sudden enlargement, accompanied by abrupt

**FIG. 2** Coefficient of entrance head loss, $K_{ent}$; redrawn after Okiishi et al. (2006).

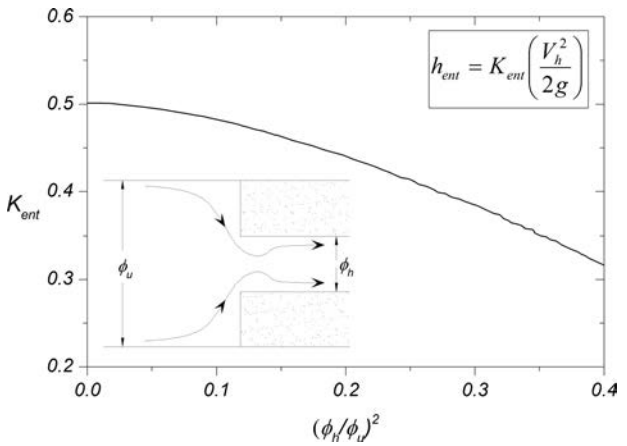

velocity decrease, which results in turbulence and velocity head loss, calculated by (Okiishi et al. 2006; Potter et al. 2011):

$$h_{ext} = K_{ext}\left(\frac{V_h^2}{2g}\right) \quad K_{ext} = \left(1 - \left(\frac{\phi_h}{\phi_d}\right)^2\right)^2 \tag{7}$$

where:

$\phi_h$ = hole diameter,

$\phi_d$ = downstream flow chamber diameter, and

$K_{ext}$ = exit head loss coefficient.

As illustrated in **Fig. 1**, $h_{ext}$ is exhausted through a horizontal distance, downstream the hole exit, beyond which the turbulence secedes, and stream velocity becomes $V_d$, that from flow rate continuity, is equal to $V_u$. Hence, $V_h^2/2g = h_{ext} + V_d^2/2g$. In HET, $\phi_h$ is significantly smaller than $\phi_d$, thus $K_{ext} \approx 1$. On the other hand, $V_d$ is insignificant considering the large $\phi_d$. Therefore for HET interpretations that require measuring downstream hydraulic conditions immediately at the hole's end, it would be convenient to say, $h_{ext} \approx V_h^2/2g$ and all the velocity head of exiting stream jet is lost (cf. **Fig. 1**).

### $h_f$ or Friction Head Loss From Stream Flow in Hole

The friction loss in the hole, $h_f$, is caused by counteracting shear stresses, i.e., $\tau_t$, that are exerted by the stream flow on the hole's peripheral walls (note: refer to the well-known Darcy-Weisbach equation). As previously stated (Eq 2), $h_f$ depends on the friction factor of hole ($f_T$ for turbulent and $f_L$ for laminar flow), that is governed primarily by $R_e$ and relative roughness of the hole's peripheral walls (Streeter et al. 1998), all which are continuously changing in an HET test.

## HET Interpretation Methods

Hitherto, different aspects of flow hydraulics in HET, and several assumptions regarding the relevancy and significance of head losses have been considered by researchers. Three main perspectives, summarized in **Table 2**, are as follows:

### Wan and Fell (2002)

It was assumed by Wan and Fell (2002) that flow velocity, i.e., $V$, in the upstream/downstream flow chambers is insignificant and negligible. Hence, $V_u^2/2g$, $V_d^2/2g$ and associated losses, i.e., $h_{ent}$ and $h_{ex}$, are excluded from hydraulic calculations, resulting in $\Delta H = \Delta h = h_f$. In this framework, termed the Hydraulic Grade Line (HGL), $\Delta H$ is measured from differential hydraulic heads measured by manometers at sidewalls of flow chambers, just upstream and downstream of test specimen (cf. **Fig. 1**).

**TABLE 2** Hydraulic considerations of HET.

| Reference | $H$ | $\Delta H = H_u - H_d$ | Connotation |
|---|---|---|---|
| Wan and Fell (2002) | $\frac{p}{\rho_w g} + z$ | $h_f$ | HGL |
| Luthi (2011) | $\frac{p}{\rho_w g} + z + \frac{V^2}{2g}$ | $h_f$ | EGL |
| Riha and Jandora (2014) | $\frac{p}{\rho_w g} + z$ | $h_f + h_{ent} + h_{ext}$ | MHGL |
| This study | $\frac{p}{\rho_w g} + z + \frac{V^2}{2g}$ | $h_f + h_{ent}$ | MEGL |

### Luthi (2011)

According to Luthi (2011) and Luthi et al. (2012), $V_u^2/2g$ and $V_h^2/2g$ are both important in hydraulic considerations. The upstream velocity, $V_u$, is determined by continuity, whilst $V_u^2/2g$ appears insignificantly small compared to the resolution of $h_u$ (cf. **Fig. 1**); however, neglecting $V_u^2/2g$ introduces significant errors at low $h_u$ accompanied with high flow rates. Contrary to this, Luthi (2011) perceived that $h_{ent}$ is insignificant and negligible. With the application of a Pitot-static tube, in close proximity to the point where the flow stream exits the hole, see **Fig. 1**, $H_d = h_d + V_h^2/2g$ is directly measured, circumventing the need to calculate $h_{ext}$. This method is termed the energy grade line (EGL), cf. **Fig. 1**, since $\Delta H = h_f$ is measured considering complete conservation of hydraulic energy, i.e., accounting for $V_u$, and $V_h$ immediately downstream.

### Riha and Jondora (2014)

Likewise, Wan and Fell (2002, 2004), Riha and Jondora (2014) considered $V_u^2/2g$ and $V_d^2/2g$ to be insignificant and negligible, that is $H = h$. However, CFD numerical simulations by Riha and Jondora (2014) revealed that for the turbulent flow entering the hole in HET, $h_{ent}$ is important and requires attention in hydraulic considerations. It was also observed by those researchers that $K_{ent}$, and in turn $h_{ent}$, depends on $\theta$ that is hole's entrance bevel-shaped angle (note that, $\theta$ is measured from the line perpendicular to hole orientation, as illustrated in **Fig. 6**). The CFD modelling results for $\phi_u = 100$ mm and $\phi_h = 6$ mm (see **Fig. 1**), suggested $K_{ent} = 0.33$ for $\theta = 80°$ and $K_{ent} = 0.27$ for $\theta = 60°$. For the stream flow exiting the hole, it was assumed that $K_{ext} \approx 1$. As seen in **Fig. 1**, in the context of this paper, the flow-hydraulics approach of Riha and Jondora (2014) is denoted as the modified hydraulic grade line (MHGL), since $\Delta H = \Delta h = h_f + h_{ent} + h_{ext}$.

## HET Testing Program

### APPARATUS CONFIGURATION

The HET apparatus designed and commissioned in this study is schematically illustrated in **Fig. 3**. The apparatus consists of a 100 mm internal-diameter test cell (length to diameter ratio of 1) and upstream/downstream flow chambers (100 mm inside diameter and 500 mm length). Contrary to many precursor studies, herein the HET setup is vertically aligned. This is beneficiary from the prospects of producing a symmetrical and regularly shaped post-test eroded hole, and precluding

**FIG. 3**

(a) Photograph, and (b) schematic illustration of HET apparatus; note: 1-upstream conical connector, 2-hole in specimen (6 mm), 3-upstream flange/baseplate, 4-soil specimen (height = 10 cm, diameter = 10 cm), 5-$h_d$ measurement (from Pitot tube), 6-$H_d$ measurement, 7-downstream flow chamber (length = 50 cm, internal diameter = 10 cm), 8-downstream conical connector, 9-outlet pipe, 10-Pitot tube, 1-$h_d$ measurement (from manometer), 12-downstream flange/baseplate, 13-wire grid (6.7 mm aperture, 30 mm circular central opening), 14-poly(methyl methacrylate) (PMMA) cylinder (2 cm wall thickness), 15-$h_u$ measurement (from manometer), 16-downstream flow chamber (length = 50 cm, internal diameter = 10 cm), 17-inlet pipe.

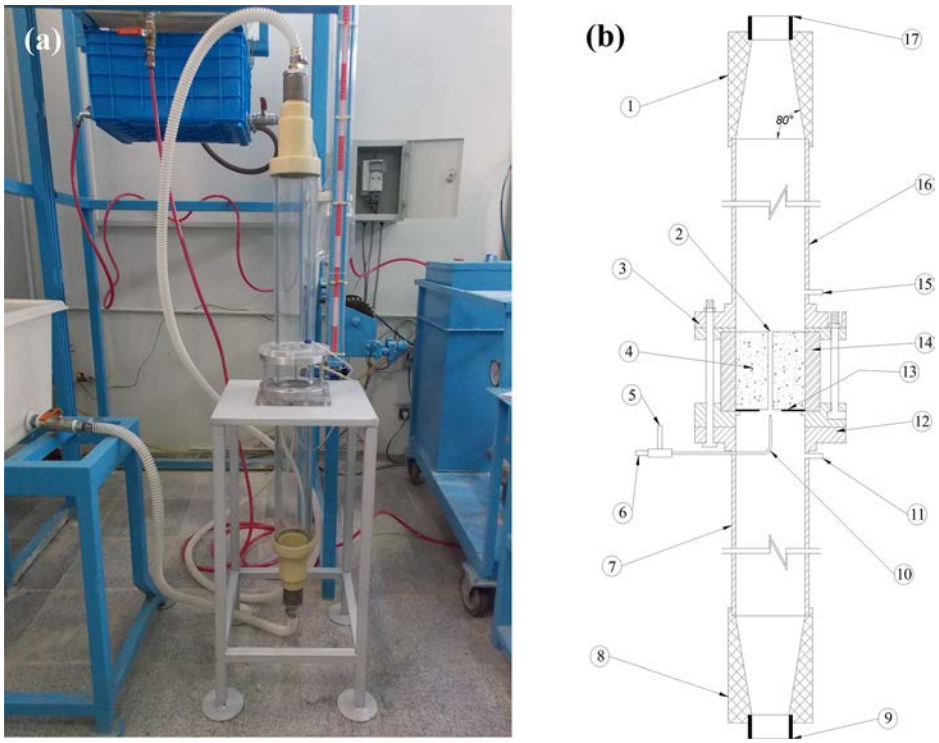


accumulation of eroded mass and air entrapment in the hole. Concerns about the mechanical stability of the vertical HET specimen are mitigated by utilizing a bottom wire grid (cf. **Fig. 3**).

A Pitot-static tube is installed at the downstream hole end (cf. **Fig. 3**). The experimental setup uses manual flow rate (by stopwatch and graduated cylinder) and head (using standpipes) measurements. The water flow is provided by a variable-elevation constant-head tank, with maximum applicable *test head* of 3500 mm (note that; *test head* is neither $H_u$ nor $h_u$, but rather the constant-head of water provided by the variable-elevation tank during testing stages). The upstream/downstream flow chambers are fabricated from transparent poly(methyl methacrylate) (PMMA), thus enabling qualitative assessment of emerging effluent turbidity with guides similar to pinhole dispersion test (ASTM D4647/D4647M-13).

## MATERIALS SPECIFICATIONS

The fine grained soils selected for testing were acquired from core material borrows of several embankment dams currently under construction in Iran. The gradation curves and properties of tested soils are presented in **Fig. 4** and **Table 3**, respectively. All soil samples had a maximum size of 4.75 mm (cf. **Fig. 4**); i.e. about $^1/_{21}$ cell diameter, which fits well in limits suggested for the permeameter test (ASTM D2434-68(2006)). Erosion tests were carried out using tap water, with average total dissolved solids (TDS) of 300–400 mg/l, dissolved oxygen (DO) around 6 mg/l, electric conductivity (EC) of about 0.1 µs/cm, and pH of 6.5–8.5. The water temperature in all tests was from 18 to 20°C.

## TESTING PROCEDURE AND INTERPRETATION METHOD

Soil specimens were moisturized to target water content and stored overnight in plastic bags for curing. Test specimens were reconstituted in four layers inside the cell using a standard compaction hammer, while exercising an under-compaction scheme (Ladd 1978) to insure even compaction throughout the specimen's length, in order to prevent possible cavities (i.e., necking) in the hole upon erosion (Lim 2006). A 6 mm-diameter hole was carefully drilled along the specimen's longitudinal axis, using a sharp auger.

The test cell is affixed in the apparatus, between the upstream and downstream flow chambers, and manometer pipes/connections are installed. The system is then de-aerated very slowly by a minute upward flow of water. The test is started after the upstream constant head tank is adjusted to provide the initial test head of 200 mm, and manometer valves are opened. Elapsed time, manometers readings, flow rate, and water temperature are recorded every 1–2 minutes.

Whenever the hole experiences no erosion (noticed from effluent turbidity and constant flow rate), the *test head* is increased (by raising the upstream constant head tank)—usually doubled unless there are reasons to believe that critical

**FIG. 4**
Gradations of core soils samples.

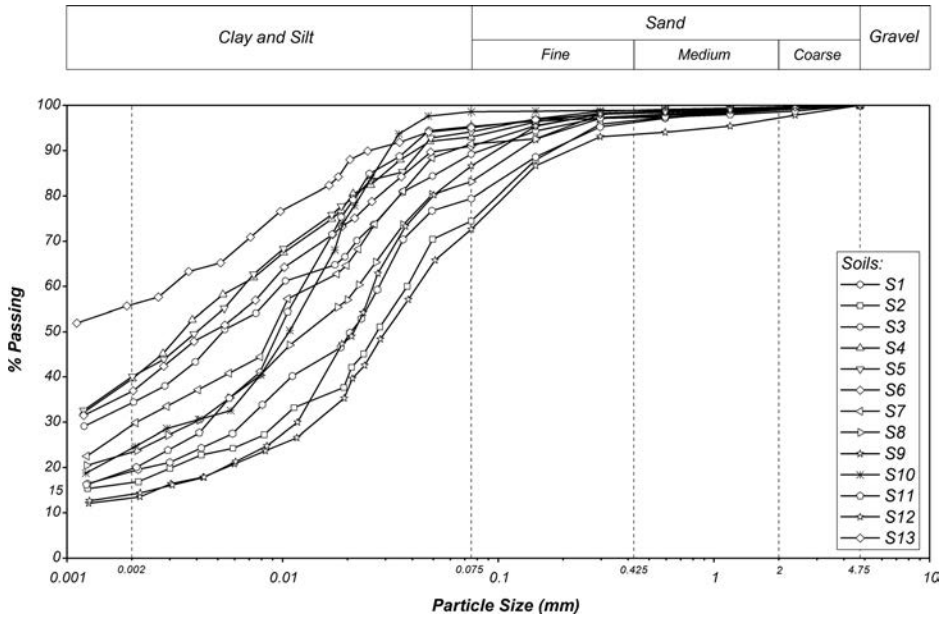


conditions may occur at an intermediate level. If the flow rate increases, the *test head* is maintained until the test completion (Luthi 2011).

The test is terminated (by closing the downstream valve) upon observing one of the following conditions: several minutes of accelerating flow, no noticeable erosion in one hour at maximum test head, and severe erosion with hole enlargement, reaching walls of test cell (Luthi 2011). Finally, the apparatus is drained from the bottom and dismantled.

**TABLE 3** Properties of tested core soil samples.

| | | Atterberg Limits[b] | | Compaction Specifications[c] | | Dispersivity |
|---|---|---|---|---|---|---|
| Soil | USCS[a] | LL (%) | PI (%) | $\rho_{dmax}$ (kg/m$^3$) | $w_{opt}$ (%) | Dispersion %[d] |
| S1 | CL | 24.4 | 8.4 | 1870 | 14.3 | 23.1 |
| S2 | CL-ML | 22.4 | 6.4 | 1840 | 13.6 | 23.8 |
| S3 | CL | 38.7 | 19.3 | 1690 | 18.3 | 18.4 |
| S4 | CL | 41.8 | 21.2 | 1650 | 19.0 | 26.1 |
| S5 | CL | 42.0 | 19.4 | 1650 | 20.3 | 25.4 |
| S6 | CL | 35.0 | 15.5 | 1700 | 19.0 | 18.9 |
| S7 | CL | 26.6 | 10.7 | 1820 | 14.8 | 23.3 |
| S8 | CL | 25.5 | 9.3 | 1860 | 13.2 | 26.4 |
| S9 | CL-ML | 20.8 | 4.0 | 1960 | 12.0 | 21.1 |
| S10 | CL-ML | 27.0 | 7.1 | 1870 | 13.4 | 57.8 |
| S11 | CL-ML | 26.5 | 5.7 | 1780 | 16.7 | 61.2 |
| S12 | CL-ML | 22.7 | 5.3 | 1890 | 13.2 | 15.9 |
| S13 | CH | 73.0 | 39.7 | 1430 | 26.1 | 70.0 |

[a]Unified Soil Classification System.
[b]ASTM D4318-10e1.
[c]ASTM D698-12e2;
[d]ASTM D4221-11.

Possible shortening, in length of eroded hole during testing, is assumed to be linearly related with elapsed time (Farrar et al. 2007; Wahl et al. 2008a).

Test interpretations were predicated on a new method devised by the authors, termed the modified energy grade line (MEGL), which in essence combines aspects of EGL and MHGL methods (see HET Interpretation Methods). As illustrated in **Fig. 1** and stated in **Table 2**, in this methodology: (*i*) $h_d + V_h^2/2g$ is directly measured (by Pitot-tube) at the hole's exit, alleviating the need to consider $h_{ext}$; (*ii*) $H_u = h_u + V_u^2/2g$ where $V_u$ is defined from flow-rate continuity; and (*iii*) $h_{ent}$ is considered in the overall head losses.

Recalling the computational analysis by Riha and Jandora (2014), a relatively accurate estimate of $h_{ent}$ requires considering the bevel-shaped entrance (to the hole). For this reason, the bevel-shaped entrance angle, $\theta$, is carefully measured after each test; that is, after disassembling the apparatus, the hole is carefully photographed, then filled with molten wax, which after setting/solidification assists in diameter/shape measurement. With the aide of $\theta$, a rational estimation of $K_{ent}$ is made, which defines $h_{ent}$ and subsequent calculations.

With reference to **Fig. 5**, calculation of erodibility characteristics for soils, i.e., $\tau_c$ and $C_e$, requires the following steps:

- In the plot of test head and Q, versus time, initiation of accelerating flow is determined as where Q starts to increase in a constant test head (cf. **Fig. 5a**).
- A polynomial curve is fitted to portion of $\phi_t - t$ variation with accelerating flow (see **Fig. 5b**). Whenever the initial test head is insufficient to cause immediate erosion, yet progressive erosion begins at further time without any head increase, it is most effective to fit a third order polynomial function to $\phi_t - t$. This leads to a parabolic $\dot{\varepsilon}_t - \tau_t$

**FIG. 5**

Calculation of erosion characteristics, i.e., $\tau_c$ and $C_e$, from HET; (a) test head and flow rate, Q, versus elapsed time, (b) variation of hole diameter, $\phi_t$, with elapsed time, and (c) relation between erosion rate, $\dot{\varepsilon}_t$, and exerted boundary shear stress, $\tau$.

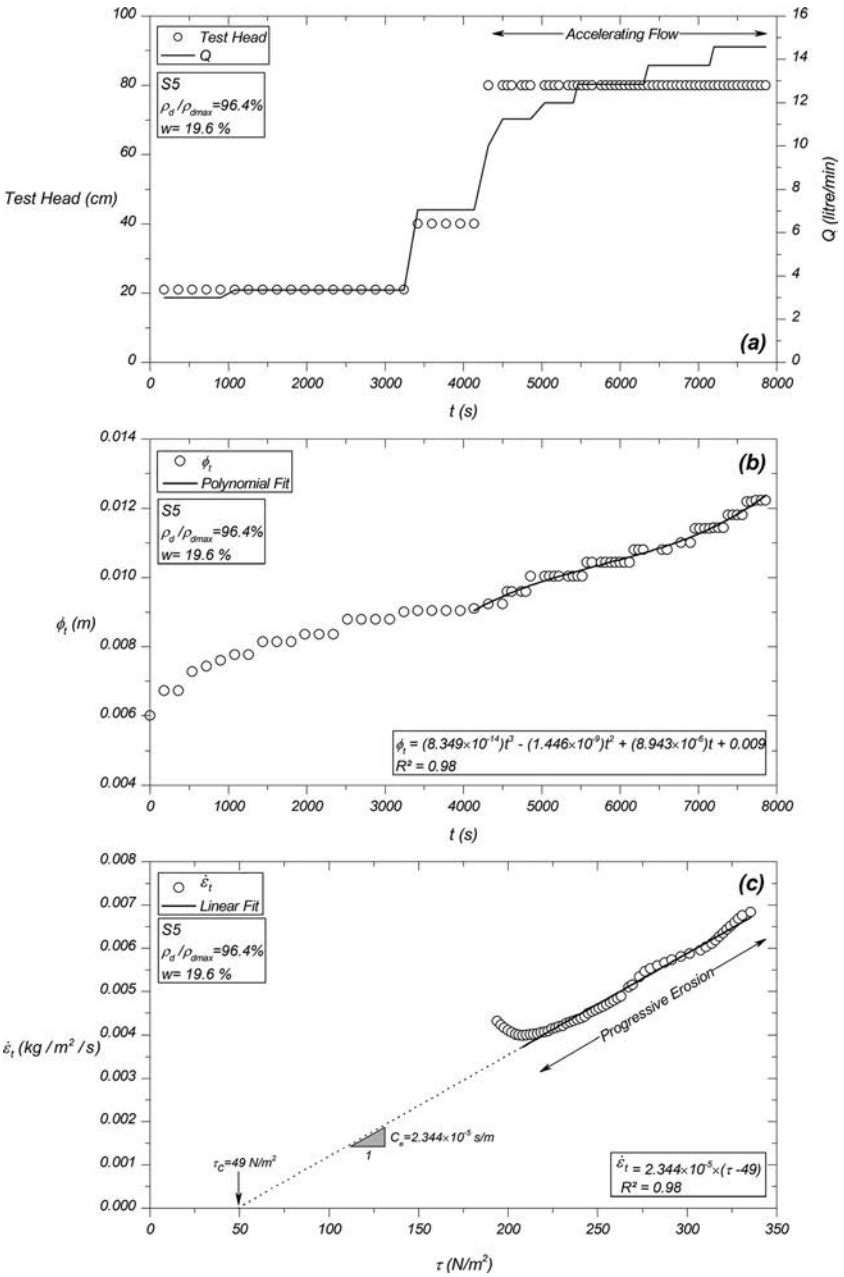


variation. When the initial test head causes immediate progressive erosion, a second order polynomial is more realistic to model $\phi_t - t$, resulting in linear variation for $\dot{\varepsilon}_t - \tau_t$ (Wahl et al. 2008a, 2008b).

- As seen in **Fig. 5c**, a straight line approximates the raising portion of $\dot{\varepsilon}_t - \tau_t$ variation, i.e. progressive erosion. From this, $C_e$ is the slope and $\tau_c$ is the horizontal intercept.

## Results and Observations

The HET test specifications for 13 core soils are presented in **Table 4**. Test specimens were reconstituted with compaction ratio, i.e., $\rho_d/\rho_{dmax}$, from 93 to 98 %, at water content of $w_{opt} \pm 2$ %.

During the test, it was observed that in specimens with low erosion resistance, the effluent is highly turbid and eroded particles are small flocculates, whereas for high erosion resistance specimens, the effluent is comparatively clearer and eroded soil is in form of large flakes/chunks.

The holes' bevel-shaped entrance angles, $\theta$, reported in **Table 4**, are measured from the erosion pattern profiles drawn in **Fig. 6**. Specimens S12 and S13 completely collapsed, leaving no erosion pattern, almost immediately upon flow establishment. Moreover, erosion characteristics were not quantifiable

**TABLE 4** Summary of HET tests conditions.

| Specimen | $w$ (%) | $\rho_d/\rho_{d\max}$ (%) | Time (min) | $\phi_h$ @ $t_f$ (mm)[a] | $\theta$ (°)[b] | $K_{ent}$[c] |
|---|---|---|---|---|---|---|
| S1 | 14.5 | 95.7 | 11 | 17 | 65 | 0.3 |
| S2 | 14.1 | 96.1 | 33 | 13 | 78 | 0.3 |
| S3 | 18.5 | 97.2 | 120 | 10 | 69 | 0.3 |
| S4 | 19.0 | 95.7 | 105 | 9.7 | 90 | 0.49 |
| S5 | 19.6 | 96.4 | 131 | 10 | 90 | 0.49 |
| S6 | 19.6 | 95.3 | 120 | 10 | 90 | 0.49 |
| S7 | 15.3 | 97.4 | 90 | 11 | 90 | 0.49 |
| S8 | 13.3 | 95.1 | 20 | 12.7 | 90 | 0.49 |
| S9 | 12.7 | 95.3 | 9 | 19.6 | 53 | — |
| S10 | 15.2 | 95.1 | 23 | 24 | 67 | — |
| S11 | 18.5 | 94.2 | 10 | 29 | 63 | — |
| S12 | 13.3 | 95.8 | 3 | 17 | — | — |
| S13 | 26.5 | 93.9 | 3 | 13 | — | — |

[a]Hole diameter at test termination.
[b]Defined in **Fig. 6**.
[c]Entrance head loss coefficient.

for specimens S9 to S13. Such an outcome was caused by one of the following conditions: (i) the hole collapsed almost immediately upon flow establishment. Apparently, the initial low flow rate was unable to remove collapsed soil debris; hence, the hole was blocked and test continuation was impossible. (ii) The hole was not blocked, yet very rapid specimen erosion occurred, insomuch as upstream and downstream manometer levels quickly converged (i.e., equalized) in short time (about 4–5 min); hence, head difference was undetectable, rendering calculation schemes inapplicable.

Soils S10, S11, and S13 are dispersive (cf. **Table 3**) and this is the reason for their quick disintegration. Soils S9 and S12 are low plasticity silts (CL-ML), which easily soften upon contact with water.

For specimens S1, S2, and S3, $\theta$ is between 60° and 80° (cf. **Table 4**), moreover, according to **Fig. 2** and the final hole diameters, $\phi_h$, reported in **Table 4**, little variation in $K_{ent}$ is expected. Therefore, from the numerical results of Riha and Jandora (2014), $K_{ent} = 0.3$ would be a fair estimate (see HET Interpretation Methods). In case of soils S4 to S8, the hole entrance in eroded specimens was not bevel-shaped implying

**FIG. 6**
Erosion patterns of specimens after HET tests.

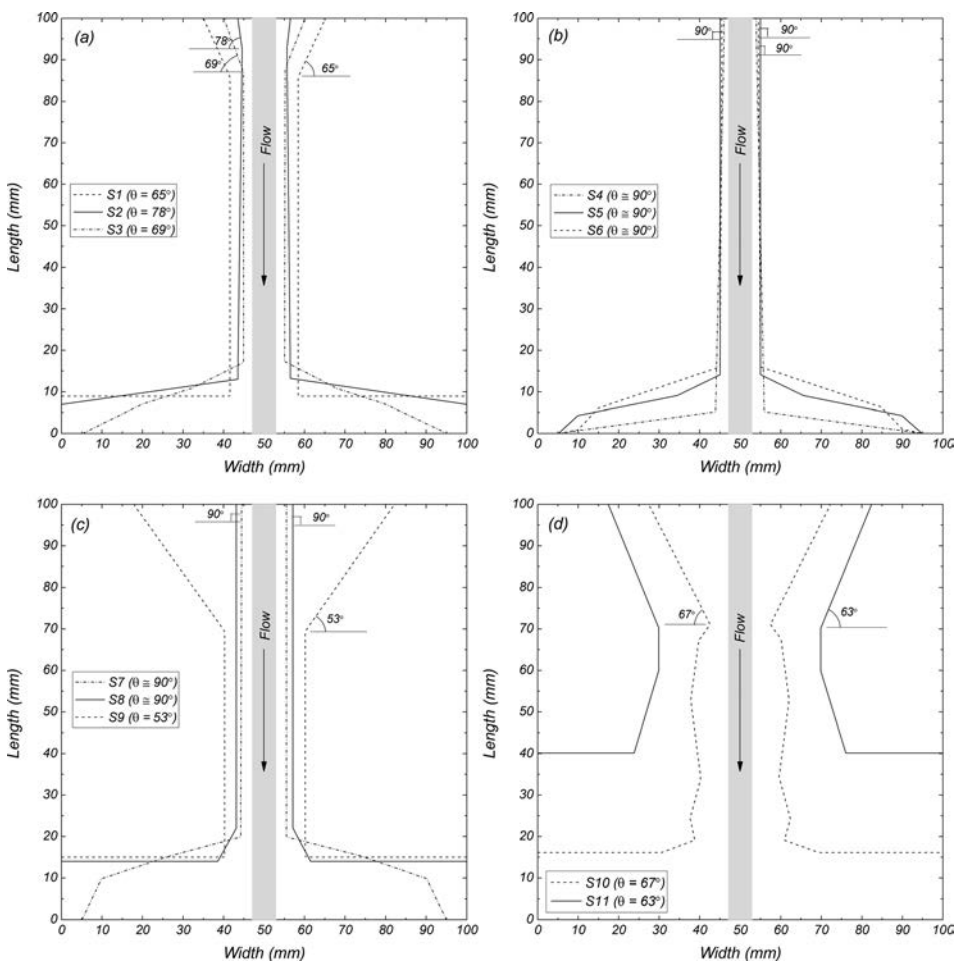

**TABLE 5** Summary of HET results from different interpretation approaches.

| | HGL | | | | EGL | | | | MEGL | | | |
|---|---|---|---|---|---|---|---|---|---|---|---|---|
| Soil | $\tau_c$ (N/m$^2$) | $C_e$ ($\times 10^{-5}$) (s/m) | $I$ | Group | $\tau_c$ (N/m$^2$) | $C_e$ ($\times 10^{-5}$) (s/m) | $I$ | Group | $\tau_c$ (N/m$^2$) | $C_e$ ($\times 10^{-5}$) (s/m) | $I$ | Group |
| S1 | 10.33 | 501.19 | 2.30 | 2 | 9.11 | 446.68 | 2.35 | 2 | 9.02 | 125.89 | 2.90 | 2 |
| S2 | 20.40 | 19.95 | 3.70 | 3 | 15.93 | 95.45 | 3.02 | 3 | 13.00 | 70.00 | 3.15 | 3 |
| S3 | 110.00 | 1.58 | 4.80 | 4 | 83.30 | 1.86 | 4.73 | 4 | 70.00 | 2.00 | 4.70 | 4 |
| S4 | 115.00 | 2.24 | 4.65 | 4 | 68.11 | 2.82 | 4.55 | 4 | 50.00 | 3.00 | 4.52 | 4 |
| S5 | 125.00 | 1.26 | 4.90 | 4 | 69.94 | 2.00 | 4.70 | 4 | 49.00 | 2.34 | 4.60 | 4 |
| S6 | 160.00 | 1.00 | 5.00 | 5 | 98.52 | 0.30 | 5.52 | 5 | 83.33 | 0.93 | 5.03 | 5 |
| S7 | 34.00 | 19.95 | 3.70 | 3 | 24.25 | 17.78 | 3.75 | 3 | 21.00 | 30.00 | 3.52 | 3 |
| S8 | 18.21 | 79.43 | 3.10 | 3 | 12.75 | 44.67 | 3.35 | 3 | 10.95 | 70.79 | 3.15 | 3 |

Note: Group number based on **Table 1**.

that $\theta \approx 90°$. Considering $\phi_h/\phi_u$ for such specimens, $K_{ent} = 0.49$ is discernible from **Fig. 2**.

The HET results from different interpretation approaches are presented in **Table 5**. Accordingly, although differences are observed between $C_e$ and $\tau_c$ from different methods, the erosion rate indices, $I$, are close, in so far as all interpretation methods classify the soil in an identical group of **Table 1**.

The variations of critical shear stresses, $\tau_c$, obtained from MEGL (i.e., $\tau_{c,ME}$), EGL (i.e., $\tau_{c,E}$), and HGL (i.e. $\tau_{c,H}$) methods are shown in **Fig. 7**. Generally, speaking differences between $\tau_{c,ME}$ and $\tau_{c,H}$ increases with increase of $\tau_c$. Moreover, $\tau_{c,ME}/\tau_{c,H}$ ranges from 0.39 to 0.87 with the best trend of $\tau_{c,ME}/\tau_{c,H} = 0.5$ (see **Fig. 7a**). Interestingly, numerical computations by Riha and Jandora (2014) for critical shear stresses in the MHGL method, i.e., $\tau_{c,MH}$, had suggested that $\tau_{c,MH}/\tau_{c,H} = 0.52$–$0.6$, where "This holds for relatively small discharges and velocities in the hole, and for higher discharges the difference can be even greater" (Riha and Jandora 2014). The results of this study comply well with the results of Riha and Jandora (2014), since inherently the only difference between the MHGL and MEGL methods, is consideration of the small $V_u^2/2g$ in the latter approach.

As illustrated in **Fig. 7b**, $\tau_{c,ME}/\tau_{c,E}$ ranges from 0.70 to 0.99 with the best trend of $\tau_{c,ME}/\tau_{c,E} = 0.8$, and the divergence from $\tau_{c,ME} = \tau_{c,E}$ is more pronounced at higher $\tau_c$. This observation is foreseeable, since EGL and MEGL methods are identical, except for the latter considering $h_{ent}$.

Overall, for soils with low erosion resistance $I < 3$, $\tau_{c,ME}$, $\tau_{c,E}$, and $\tau_{c,H}$ are very close. With the increase in specimen erosion resistance, i.e., soils with $I > 3$ according to **Table 1**, differences of $\tau_{c,ME}$, $\tau_{c,E}$, and $\tau_{c,H}$ increase.

Considering soils for which HET is unfeasible (e.g., S9 to S13), Wahl et al. (2008a) state that the HET "in its current configuration cannot provide a quantitative measure of the erodibility of many materials in groups 1–2 and 5–6," and the lowest $I$ reported by those authors was 2.45. In **Table 5**, the lowest $I$, calculated from the HGL method, is 2.3 observed for soil S1.

A guide to estimating erosion properties of soils for which HET is unfeasible, is using precursor experiences, similar to those provided by Wan and Fell (2002). Accordingly, for non-dispersive SM, SC, ML, and CL-ML soils the erosion rate index, $I$, is about 2 to 3. It may, therefore, be concluded that when HET is unfeasible for highly erodible soils, the erosion rate index, $I$, would most probably be less than 2.

**FIG. 7**

Graph of critical shear stress variations; (a) MEGL ($\tau_{c,ME}$) versus HGL ($\tau_{c,H}$), and (b) MEGL ($\tau_{c,ME}$) with respect to EGL ($\tau_{c,E}$).

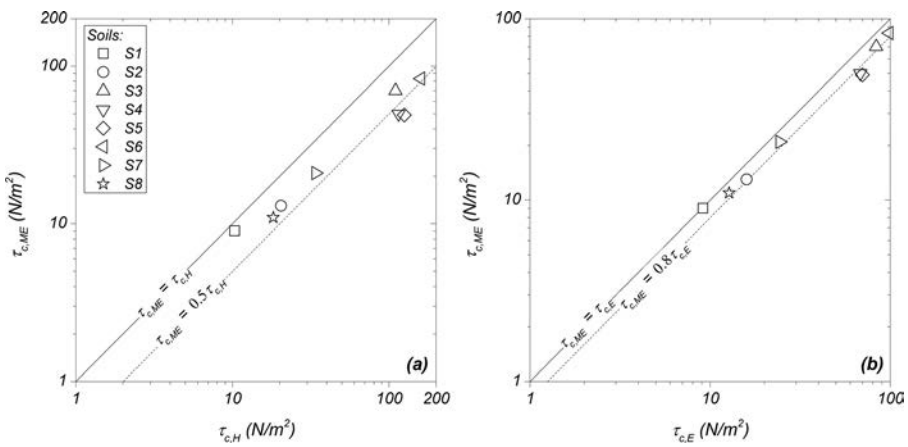

## Summary Remarks and Conclusions

The HET test has been introduced a decade ago; nevertheless, a unified and standardized method for conducting and interpreting HET is not yet available. This is disquieting noticing that the HET is now widely accepted as a routine test for measuring soil erodibility characteristics, both for research and real engineering projects/services.

This paper presented refinements to calculating/measuring the water head drop, $h_f$, in the HET. A new approach was proposed and compared with three previous HET analysis methods, through analyzing erosion characteristics of 13 fine-grained soils.

Test results and observations suggest that soils with high erosion resistance reflect higher difference in critical shear stresses, $\tau_c$, obtained by hydraulic grade line method (HGL), energy grade line method (EGL), and modified energy gradient line method (MEGL). Moreover, $\tau_{c,ME}/\tau_{c,H}$ ranges from 0.39 to 0.87 with the best trend of $\tau_{c,ME}/\tau_{c,H} = 0.5$ and $\tau_{c,ME}/\tau_{c,E}$ ranges from 0.70 to 0.99 with the best trend of $\tau_{c,ME}/\tau_{c,E} = 0.8$, and the divergence from $\tau_{c,ME} = \tau_{c,E}$ is more pronounced at higher $\tau_c$.

Values of the erosion rate indices, $I$, obtained from HGL, EGL, and MEGL are close, and the associated group number is identical. Therefore, the erosion rate index reliably manifests soil erosion propensity.

### ACKNOWLEDGMENTS

The constructive comments, both technical and editorial, by the anonymous reviewers are gratefully acknowledged. The writers would like to express their gratitude to Professor A. R. Zarrati for his comments on pipe-flow hydraulics. Also, the kind efforts of Mr. Reza Javadi for providing help and assistance during testing is appreciated.

## References

ASTM D698-12e2, 2012, *Standard Test Method for Laboratory Compaction Characteristics of Soil Using Standard Effort*, ASTM International, West Conshohocken, PA, www.astm.org

ASTM D2434-68(2006), 2006, *Standard Test Method for Permeability of Granular Soils (Constant Head)*, ASTM International, West Conshohocken, PA, www.astm.org

ASTM D4221-11, 2011, *Standard Test Method for Dispersive Characteristics of Clay Soil by Double Hydrometer*, ASTM International, West Conshohocken, PA, www.astm.org

ASTM D4318-10e1, 2010, *Standard Test Methods for Liquid Limit, Plastic Limit, and Plasticity Index of Soils*, ASTM International, West Conshohocken, PA, www.astm.org

ASTM D4647/D4647M-13, 2013, *Standard Test Method for Identification and Classification of Dispersive Clay Soils by the Pinhole Test*, ASTM International, West Conshohocken, PA, www.astm.org

Benahmed, N. and Bonelli, S., 2012, "Investigating Concentrated Leak Erosion Behaviour of Cohesive Soils by Performing Hole Erosion Tests," *Eur. J. Environ. Civ. Eng.*, Vol. 16, No. 1, pp. 43–58, http://dx.doi.org/10.1080/19648189.2012.667667

Benahmed, N. and Bonelli, S., 2012, "Internal Erosion of Cohesive Soils: Laboratory Parametric Study," presented at the *6th International Conference on Scour and Erosion*, Paris, France, August 27–31, ICSE, Paris, France, pp. 1041–1047.

Bonelli, S., Ed., 2013, *Erosion in Geomechanics Applied to Dams and Levees*, John Wiley & Sons, New York.

Bonelli, S., Brivois, O., Borghi, R., and Benahmed, N., 2006, "On the Modelling of Piping Erosion," *Comptes Rendus Mécanique*, Vol. 334, Nos. 8–9, pp. 555–559, http://dx.doi.org/10.1016/j.crme.2006.07.003

Bonelli, S. and Brivois, O., 2008, "The Scaling Law in the Hole Erosion Test With a Constant Pressure Drop," *Int. J. Numer. Anal. Methods Geomech.*, Vol. *32*, No. 13, pp. 1573–1595, http://dx.doi.org/10.1002/nag.683

Boukhemacha, M., 2009, "A Hole Erosion Test Model A Step on Internal Erosion Modeling," *Sci. Bull. Ser.: Math. Modell. Civ. Eng.*, Vol. 5, No. 3, pp. 17–24, http://dx.doi.org/10.3311/PPee.2145

Boukhemacha, M. A., Bica, I., and Mezouar, K., 2013, "New Procedures to Estimate Soil Erodibility Properties From a Hole Erosion Test Record," *Period. Polytech. Civ. Eng.*, Vol. *57*, No. 1, pp. 77–82.

Chevalier, C., Haghighi, I., Pham, T. L., Reiffsteck, P., Burns, S. E., Bhatia, S. K., Avila, C. M. C., and Hunt, B. E., 2011, "Two Complementary Tests for Characterizing the Soil Erosion," presented at *Scour and Erosion. Proceedings of the Fifth International Conference on Scour and Erosion (ICSE-5)*, San Francisco, CA, November 7–10, ASCE, Reston, VA, pp. 152–161.

Chevalier, C., Haghighi, I., and Herrier, G., 2012, "Resistance to Erosion of Lime Treated Soils: A Complete Parametric Study in Laboratory," presented at the *6th International Conference on Scour and Erosion*, Paris, France, August 27–31, ICSE, Paris, France, pp. 161–168.

Farrar, J. A., Torres, R. L., and Erdogan, Z., 2007, "Bureau of Reclamation Erosion Testing for Evaluation of Piping and Internal Erosion of Dams," presented at the *Geo-Denver2007: New Peaks in Geotechnics*, Denver, CO, February 18–21, ASCE, Reston, VA, pp. 22–31.

Foster, M., Fell, R., and Spannagle, M., 2000, "A Method for Assessing the Relative Likelihood of Failure of Embankment Dams by Piping," *Can. Geotech. J.*, Vol. 37, No. 5, pp. 1025–1061, http://dx.doi.org/10.1139/t00-029

Haghighi, I., Chevalier, C., Duc, M., Guédon, S., and Reiffsteck, P., 2012, "Improvement of Hole Erosion Test and Results on Reference Soils," *J. Geotech. Geoenviron. Eng.*, Vol. 139, No. 2, pp. 330–339, http://dx.doi.org/10.1061/(ASCE)GT.1943-5606.0000747

ICOLD, 2013, "Internal Erosion of Existing Dams, Levees and Dykes, and Their Foundations," *Bulletin 164, Volume 1: Internal Erosion Processes and Engineering Assessment*, International Commission on Large Dams, Paris, France.

ICOLD, 2016, "Internal Erosion in Existing Dams, Dikes and Levees and Their Foundations," *Bulletin 164 Volumes 2: Case Histories, Investigations, Testing, Remediation and Sur-*

*veillance*, International Commission on Large Dams, Paris, France.

Kissi, B., Vera, M. A. P., Cintas, M. R., and Khamlichi, A., 2012, "Modeling the Fluid/Soil Interface Erosion in the Hole Erosion Test," presented at the *MATEC Web of Conferences*, *Volume 1, CSNDD 2012 International Conference on Structural Nonlinear Dynamics and Diagnosis*, M. Belhaq and R. Ibrahim (Eds.), Marrakech, Morocco, April 30–May 2, 2012, Article No.: 00003, Published by EDP Sciences- France, 17 Avenue du Hoggar, Parc d'Activité de Courtabuf, BP 112, 91944 Les Ulis Cedex A, France, http://dx.doi.org/10.1051/matecconf/20120100003

Ladd, R. S., 1978, "Preparing Test Specimens Using Undercompaction," *Geotech. Test. J.*, Vol. *1*, No. 1, pp. 16–28.

Lim, S. S., 2006, "Experimental Investigation of Erosion in Variably Saturated Clay Soils," Ph.D. thesis, The University of New South Wales, NSW, Australia.

Luthi, M., 2011, "A Modified Hole Erosion Test (HET-P) to Study Erosion Characteristics of Soil," Ph.D. thesis, The University of British Columbia, Vancouver, BC.

Luthi, M., Fannin, R. J., and Millar, R. G., 2012, "A Modified Hole Erosion Test (HET-P) Device," *Geotech. Test. J.*, Vol. 35, No. 4, pp. 660–664, https://doi.org/10.1520/GTJ104336

Marot, D., Regazzoni, P. L., and Wahl, T., 2011, "Energy-Based Method for Providing Soil Surface Erodibility Rankings," *J. Geotech. Geoenviron. Eng.*, Vol. 137, No. 12, pp. 1290–1293, http://dx.doi.org/10.1061/(ASCE)GT.1943-5606.0000538

Mercier, F., Bonelli, S., Golay, F., Anselmet, F., Philippe, P., and Borghi, R., 2015, "Numerical Modelling of Concentrated Leak Erosion During Hole Erosion Tests," *Acta Geotech.*, Vol. 10, No. 3, pp. 319–332, http://dx.doi.org/10.1007/s11440-014-0349-5

Okiishi, M. Y., Munson, B., and Young, D., 2006, *Fundamentals of Fluid Mechanics*, John Wiley & Sons, Inc., New York.

Potter, M., Wiggert, D., and Ramadan, B., 2011, *Mechanics of Fluids SI Version*, Cengage Learning, Boston, MA.

Reiffsteck, P., Pham, T. L., Vargas, R., and Paihua, S., 2006, "Comparative Study of Superficial and Internal Erosion Test," *Proceedings 3rd International Conference on Scour and Erosion (ICSE-3)*, Verheij, H.J. and Hoffmans G.J.C.M. (Eds.), November 1–3, 2006, CURNET, Gouda, Amsterdam, The Netherlands, pp. 571–575.

Regazzoni, P. L. and Marot, D., 2013, "A Comparative Analysis of Interface Erosion Tests," *Nat. Hazards*, Vol. 67, No. 2, pp. 937–950, http://dx.doi.org/10.1007/s11069-013-0620-3

Říha, J. and Jandora, J., 2014, "Pressure Conditions in the Hole Erosion Test," *Can. Geotech. J.*, Vol. 52, No. 1, pp. 114–119, http://dx.doi.org/10.1139/cgj-2013-0474

Streeter, V. L., Wylie, E. B., and Bedford, K. W., 1998, *Fluid Mechanics*, McGraw-Hill, New York.

Wahl, T. L., Regazzoni, P. L., and Erdogan, Z., 2008a, *Determining Erosion Indices of Cohesive Soils With the Hole Erosion Test and Jet Erosion Test*, US Department of Interior, Bureau of Reclamation, Technical Service Center, Washington, D.C.

Wahl, T. L., Erdogan, Z., and Kepler, W. F., 2008b, *Results of Laboratory Physical Properties and Hole Erosion Tests, Truckee Canal Embankment Breach, Newlands Project, Nevada*, US Department of Interior, Bureau of Reclamation, Technical Service Center, Washington, D.C.

Wan, C. F. and Fell, R., 2002, "Investigation of Internal Erosion and Piping of Soils in Embankment Dams by the Soil Slot Erosion Test and the Hole Erosion Test," *Report No. R-412,* University of New South Wales, School of Civil and Environmental Engineering, NSW, Australia.

Wan, C. F. and Fell, R., 2004a, "Investigation of Rate of Erosion of Soils in Embankment Dams," *J. Geotech. Geoenviron. Eng.*, Vol. 130, No. 4, pp. 373–380, http://dx.doi.org/10.1061/(ASCE)1090-0241(2004)130:4(373)

Wan, C. F. and Fell, R., 2004b, "Laboratory Tests on the Rate of Piping Erosion of Soils in Embankment Dams," *Geotech. Test. J.*, Vol. 27, No. 3, pp. 295–303, https://doi.org/10.1520/GTJ11903